SMASIS2020-2439

REAL-TIME MODEL UPDATING ALGORITHM FOR STRUCTURES EXPERIENCING HIGH-RATE DYNAMIC EVENTS

Seong Hyeon Hong
Department of Mech. Engineering
University of South Carolina
Columbia, South Carolina 29208

Claire Drnek
Department of Mech. Engineering
University of South Carolina
Columbia, South Carolina 29208

Austin Downey
Department of Mech. Engineering
Department of Civil and Env. Engineering
University of South Carolina
Columbia, South Carolina 29208

Yi Wang
Department of Mech. Engineering
University of South Carolina
Columbia, South Carolina 29208

Jacob Dodson
Air Force Research Lab (AFRL/RWMF)
Niceville, Florida 32542

ABSTRACT

Real-time model updating of active structures subject to unmodeled high-rate dynamic events require structural model updates on the timescale of 2 ms or less. Examples of active structures subjected to unmodeled high-rate dynamic events include hypersonic vehicles, active blast mitigation, and orbital infrastructure. Due to the unmodeled nature of the events of interest, the real-time model updating algorithm should circumvent any model pre-calculations. In this work, we present a methodology that updates the finite element analysis (FEA) model of a structure experiencing varying dynamics through online measurements. The algorithm is demonstrated for a testbed, comprised of a cantilever beam and a roller that serves as movable support. The structure's state is updated (i.e. the position of the moving roller) by continuously updating the associated FEA model through an online adaptive meshing and search algorithm. The structure's state is continuously estimated by comparing the measured signals with FEA models. New FEA models are built based on the enhanced estimate of the structure's state through adaptive meshing for modal analysis and adaptive search space for the FEA model selection. The proposed methodology is verified experimentally in real-time using the testbed. It is demonstrated that the adaptive features can achieve accurate state estimations within the required 2 ms timescale.

INTRODUCTION

High-rate dynamics are defined as the dynamic response of a system due to a high-rate ($<$100 ms) and high-amplitude (acceleration $>$ 100 gn) event such as a blast or impact [1]. Examples of structures that undergo high-rate dynamic events include hypersonic vehicles, active blast mitigation systems, and ballistic packages. These high-rate events are characterized by sudden and unknown changes in the magnitude and location of external loading conditions which pose a challenge when attempting to track the state of a structure. For example, active blast mitigation systems operate in order to minimize the impact of a blast or to counter the effects of the blast after impact. Because a majority of impact blasts originate from short-range threats, the response time for mitigation systems is limited. Active blast mitigation systems must be capable of detecting the presence of a blast

threat, determining the location of an incoming threat and deploy countermeasures on a millisecond timescale [2]. One approach to tracking the state of such structures is to utilize structural model updating techniques to update a digitized representation of the system state in real-time. The challenges associated with tracking the structure's state through high-rate dynamic events dictate that the model updating technique must: (1) be flexible in order to adapt and learn the changing external load conditions without relying on pre-trained data, and; (2) be capable of updating within a 2ms timescale in order to allow for decisions based on real-time data.

Real-time model updating allows for the tracking of complex structures experiencing high rate dynamics such as in-flight monitoring of manned and unmanned aerial vehicles as well as space crafts. In the case of an unmanned vehicle, a pilot is not present to monitor the aircraft and operators on the ground may not have the ability or bandwidth to process sensor readings to determine the condition of the system. Real-time model updating would allow for the almost instantaneous understanding of the structural system following an impact or other high-rate event, allowing the system to autonomously make mission-critical decisions in real-time [3]. In the case of manned vehicles and space crafts, the main goal is to protect the vehicle's occupants. However, if the system experiences damage the amount of sensor data would be overwhelming to a pilot and their reaction time would not be sufficient for making decisions. Digitized real-time models build the ground work to develop real-time decision-making software that will respond to a changing environment faster than its human occupants can [3].

Real-time online model updating has been used with non-Finite Element in order to test and simulate the response of civil structures in the past. Song et al. developed an approach utilizing the Bouc-Wen hysteresis model unscented Kalman filter to update a structure model in real-time [4]. Their approach successfully describes the non-linear state of structures experiencing loading and estimates their cyclic response for the purpose of structural health monitoring. However, real-time model updating of Finite Element Analysis (FEA) models has seen limited use due to the large computational cost associated with FEA and the difficulty of developing a mathematical model that is capable of updating on a millisecond timescale. The development of real-time model updating techniques developed for FEA models will enable further advancements in the monitoring and control of structures that experience high-rate dynamic events. Of interest to this paper, Downey et al. developed and experimentally validated a millisecond error minimization technique for FEA models that updated structures model by minimizing the error between the structure's measured state and a set of potential models calculated in real-time as the structure moved through the high-rate dynamic event [5].

Adaptive FEA is a method by which the error of a solution is calculated, and refinements are made to the mesh in order to minimize the errors. Traditionally, meshes can be refined using h-refinement or p-refinement [6]. H-refinement adjusts the size of elements within the mesh based on their location, applying smaller elements near areas of interest or where large gradients are presents, thereby increasing the number of nodes and elements. P-refinement adjusts the polynomial degree that is used to describe the structure by adding additional notes to the current number of elements. Another form of mesh refinement is r-refinement which relocates the nodes within a mesh while holding the number of nodes and elements constant and is the method of mesh refinement employed in this work [7]. R-adaptive FEA has found use mainly in 1-D fluid dynamics applications [8]. Past applications include the study of fluid through a porous medium including diffusion and filtration properties [9]. Additional applications aim to model the behavior of fluids including waves and flow past objects [10]. More recent applications include modeling shock reflection as well as objects subject to the supersonic flow through wind tunnels [11]

This paper presents and numerically validates a modified version of the ms error minimization algorithm developed by Downey et al. [5], but extended to consider an adaptive FEA formulation. As in the previous work, the algorithm seeks to update the FE models by minimizing the error between the system's measured frequency and the frequency of a series of models that are calculated in parallel and in real-time as the structure moves through the high-rate dynamic event. This paper builds on the previous work through the utilization of an adaptive FEA model that uses r- refinement which relocates the nodes withing the FEA mesh. This decreases the required computational time by reducing the complexity of the REA required to track a high-rate dynamic event in the testbed.

BACKGROUND
DROPBEAR Experimental Test Bed

This work numerically validates the proposed algorithm using a ground-truth FEA model based on the Dynamic Reproduction of Projectiles in Ballistic Environments for Advanced Research (DROPBEAR) testbed. This testbed was initially developed by Joyce et al. [12]. The motivation behind its construction was the creation of an experimental structure that was capable of repeatably altering test parameters quickly during a test. The DROPBEAR can be configured with two programmable changes, both intended to simulate damage to a structure. The first of these is a detachable mass that is attached to the structure with an electromagnet, the second of these is a movable roller boundary condition attached to a linear actuator. These programmable changes allow the DROPBEAR's cantilever beam to represent a structure experiencing a high-rate dynamic event. In this work, only the movable roller position is utilized. The configuration of the DROPBEAR considered in this work is shown in Fig. 1.
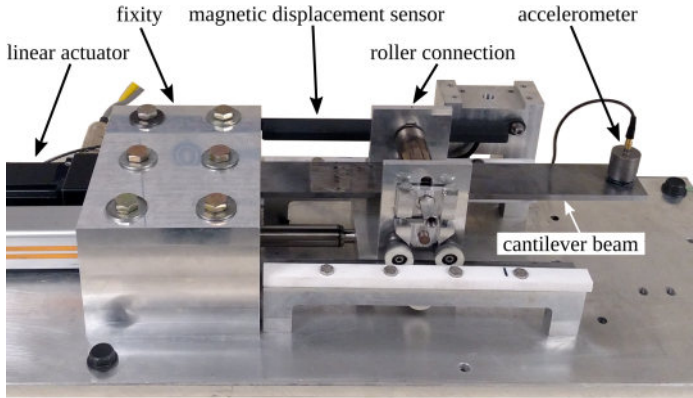
FIGURE 1. MODIFIED DROPBEAR TESTBED USED IN THIS WORK.

FIGURE 2. ROLLER TESTING PARAMETERS USED IN THIS WORK.

The DROPBEAR's current configuration features an accelerometer (PCB Piezotronics- model 393B04) mounted at the free end of a 51 x 6 x 350 mm steel cantilever beam with Density of 7800 kg/m^3, Young's Modulus of 2e11 N/m^2 and Poisson's Ratio of .26. The design also features a sliding roller cart on a linear actuator that constrains the beam between 48-175mm from the fixed end of the beam as well as a magnetic displacement sensor that measures the roller displacement throughout the test. Varying the roller location during testing can simulate damage to the system by producing a user-defined change to the testing parameters resulting in a change to the system dynamics. The use of rollers ensures the repeatability of each test, as there is no damage occurring to the beam itself, merely simulated damage. The change to the system dynamics is measured using the change in natural frequency of the beam which is obtained by taking the Fast Fourier Transform (FFT) of the data recorded by the accelerometer mounted on the free end of the beam. Before the FFT is calculated, a sliding Hann window is applied to the acceleration data to reduce the transients at the edge of the time-series data and prepare it for further processing. The data collected using DROPBEAR allows for the testing and evaluation of algorithms that model systems experiencing high-rate dynamics in real-time including the ability to detect and quantify damage that occurs to a structure using natural frequency estimation. The test profile used to define the roller location for this procedure can be seen in Fig. 2.

METHODOLOGY

This work presents a methodology that updates the FEA model of a structure in motion experiencing varying dynamics in real-time. This is done using online acquired measurements and by applying the adaptive search method to estimate the position of the moving roller. The flowchart of the proposed real-time
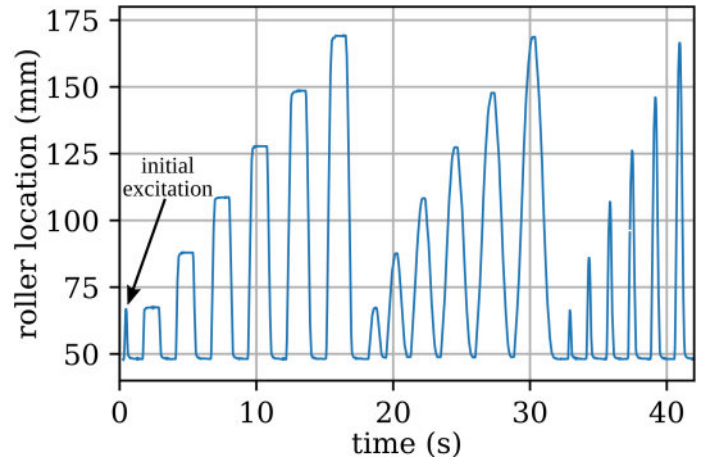
model updating scheme is displayed in Fig. 3.

The key idea is to use the FEA model to represent the high-rate dynamic system. First, we sample n roller locations following a normal probability density function (PDF) of mean, μ and standard deviation, σ. With these roller locations, n FEA models are constructed, followed by the modal analysis of all the models in parallel, yielding the first (or leading) natural frequencies of the n models ($\omega_1, \ldots, \omega_n$). The measured frequency (ω_{meas}) of the actual system, obtained using the FFT of the accelerometer signals, is then compared with ($\omega_1, \ldots, \omega_n$) to estimate the roller location. Then the PDF function utilized to sample the locations is updated based on the estimated roller location and frequency comparisons. Thus, the determination of the roller position can be continuously narrowed down by comparing the natural frequencies obtained from the experiments and from the FEA models and building new FEA models based on the enhanced estimate of the position. The entire model updating process is undertaken in real-time to monitor and track the structure as it moves through high-rate dynamic events.

FEA Model

The 1-D FEA model used to represent the system is shown in Fig. 4. As it is for the actual DROPBEAR testbed, the left end of the model is fixed and a movable support exists to represent the roller. Each element of the model adopts the Euler-Bernoulli beam theory and mesh is applied to create N elements of the beam. Consequently, there will be $N+1$ number of nodes on the beam. Two end nodes (in black) are fixed to their positions, a roller node (in green) is fixed to the roller but able to move along the beam, and all other nodes (in blue) are freely assigned. Every element is exposed to two forces and two moments as indicated from the right side of the figure. The mass (M_i) and stiffness
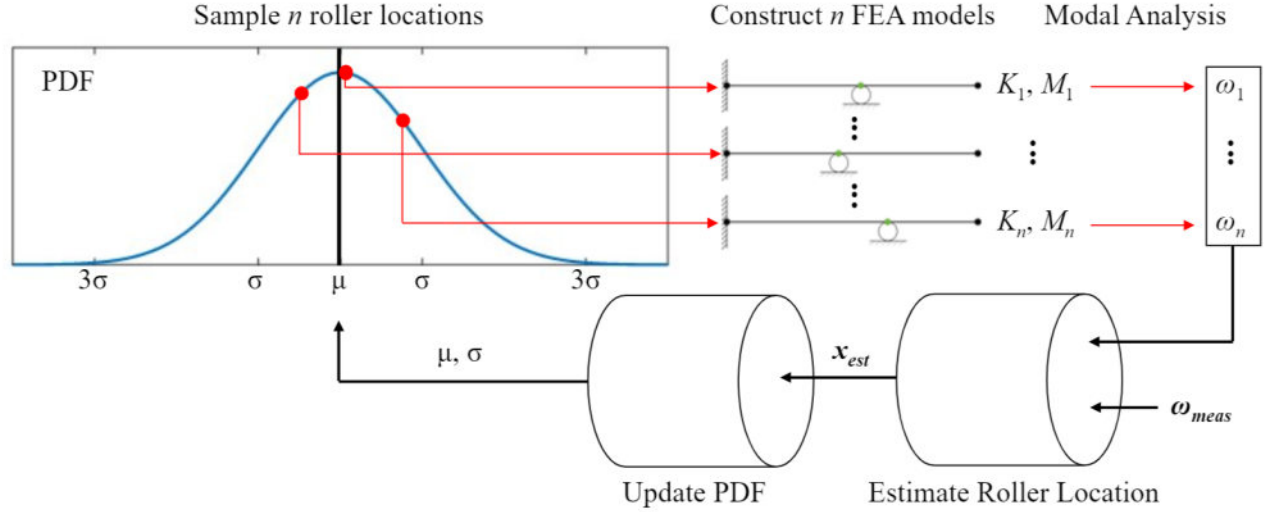
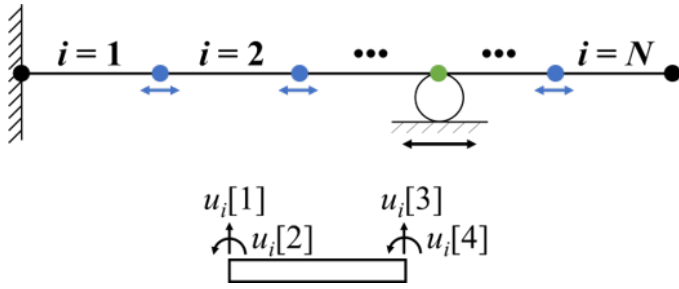**FIGURE 3**.   FLOWCHART OF THE PROPOSED REAL-TIME MODEL UPDATING.

FIGURE 4.   SCHEMATIC OF THE FEA MODEL USED IN THIS WORK.

(K_i) matrices of the element i due to these forces and moments are defined in Eqn. 1 and Eqn. 2 respectively.

$$M_i = \frac{\rho_i A_i l_i}{420} \begin{bmatrix} 156 & 22l_i & 54 & -13l_i \\ 22l_i & 4l_i^2 & 13l_i & -3l_i^2 \\ 54 & 13l_i & 156 & -22l_i \\ -13l_i & -3l_i^2 & -22l_i & 4l_i^2 \end{bmatrix}, \quad (1)$$

$$K_i = \frac{E_i I_i}{l_i} \begin{bmatrix} 12/l_i^2 & 6/l_i & -12/l_i^2 & 6/l_i \\ 6/l_i & 4 & -6/l_i & 2 \\ -12/l_i^2 & -6/l_i & 12/l_i^2 & -6/l_i \\ 6/l_i & 2 & -6/l_i & 4 \end{bmatrix} \quad (2)$$

where ρ is the density, A is the cross-sectional area, l is the length, E is the young's modulus, and I is the moment of inertia

of the beam element. These element matrices are stacked diagonally in an order to construct the global mass (M) and stiffness (K) matrices, which are then used for modal analysis to compute natural frequencies of the structure. The boundary conditions at the fixity and the roller are implemented by decimating the corresponding rows and columns of M and K matrices. As our main purpose is to update the structure experiencing high-rate dynamic events in real-time, the computation time to acquire natural frequencies of the FEA model needs to be minimized. The key idea here is to assign the smallest number of nodes while still preserving comparable accuracy with respect to a large number of nodes for the natural frequencies. In order to find the appropriate number of elements for the FEA model, convergence test has been performed when the roller is positioned at 10%, 50% (center), and 90% of the beam. At each of these locations, natural frequencies of the structure have been computed starting with 6 to 100 elements in increments of 2. The free nodes are assigned depending on the position of the roller such that the number of nodes on the left and right sides of the roller are close to evenly distributed. In other words, this is equivalent to applying adaptive mesh on the FEA model depending on the roller position. The solutions found with 1000 elements are considered as true frequencies, which are used to compute relative percentage errors of the first two natural frequencies as depicted in Fig. 5. According to the figure, for the second frequency, the discrepancy decreases as the number of elements increases. However, for the first frequency, changes are too small to be visible with bare eyes. Furthermore, we can infer that for the second frequency, the error reduction of utilizing 100 elements versus 10 elements is less than 0.1%. Therefore, 10 elements are selected to minimize the computation load. The time taken to solve for the natural fre-
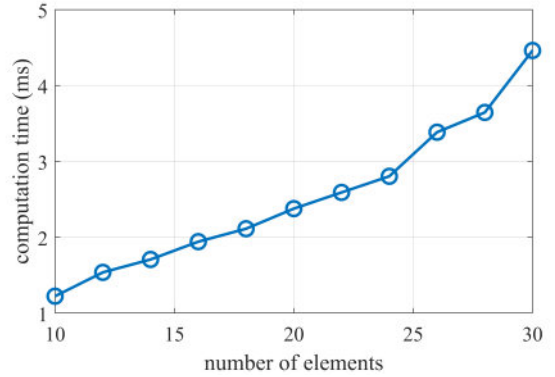
4
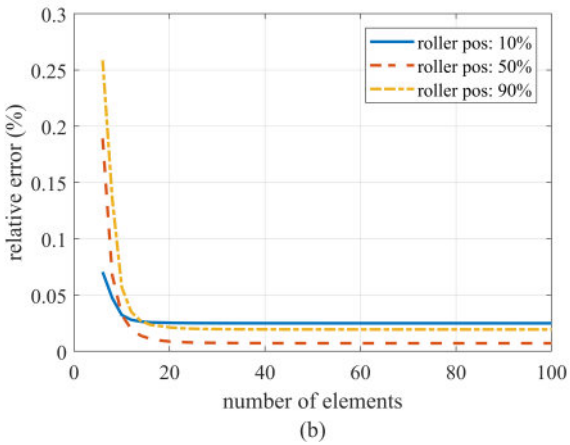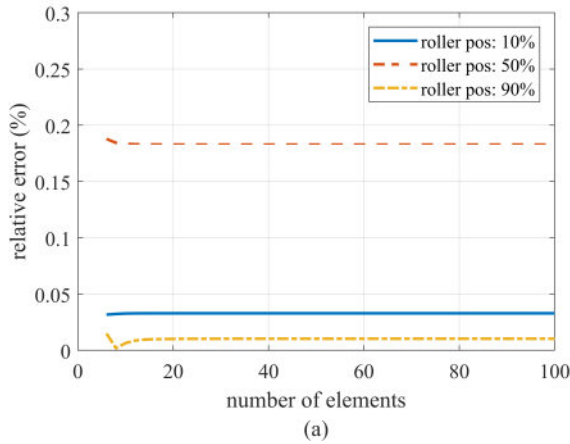
FIGURE 5. CONVERGENCES FOR THE FIRST (a) AND SECOND (b) NATURAL FREQUENCIES OF THE BEAM IN RELATIVE PERCENTAGE ERROR.

FIGURE 6. COMPUTATION TIME FOR FEA MODEL MODAL ANALYSIS.

quencies of the FEA model with different number of elements is shown in Fig. 6. For the computation, a personal computer with Intel Core i7-8700 CPU @ 3.2 GHz has been utilized. From the figure, we can infer that in order to meet the 2 ms requirement of the real-time model updating of structures experiencing high-rate dynamics, the number of elements should be strictly less than 16. Before, it was confirmed that 10 elements are enough to provide the required accuracy for the fundamental frequencies, therefore, a 10 element FEA is selected for the remainder of this work. The computation time for 10 elements is found to be approximately 1.2 ms, which provides enough time to approximate the roller location based on the found frequencies.

Estimation of Roller Location

Estimating the roller location is accomplished in two steps: (1) sampling the roller locations of the aforementioned FEA model and performing modal analysis to find natural frequencies, and (2) estimating the roller location by comparing these natural frequencies of FEA models and the measured resonant frequency from the accelerometer readings. Therefore, sampling the roller locations to create corresponding FEA models and selecting the method to estimate the roller location from the natural frequencies and a resonant frequency are vital importance in our proposed method.

In the present effort, a Gaussian distribution is utilized to sample the roller locations. The mean of the distribution function is selected to be the current estimated roller location. The initial estimated location is set to be at the center of the beam since we assume that the true initial state of the structure is unknown, which makes the center as the best guess. Selecting the appropriate standard deviation (STD) value is a big challenge since there is a trade-off between exploring and exploiting by varying the size of the search space. Here, we implement both static and dynamic STD values referred to as fixed and adaptive sampling, respectively. For fixed sampling, different STD values will be applied to illustrate the effects of the search space. On the other hand, adaptive sampling uses information to adjust the search space. For example, when the nearest sampled frequency is very different from the measured frequency, the search space needs to be expanded, that is, the roller positions used in the FEM model are distant from the actual roller position. On the contrary, it shrinks the search space when the measured frequency is close to one of the FEM-computed modal frequencies since this suggests that the sampled positions are close to the actual position, thus reducing the variance of the prediction. However, it is difficult to come up with a general rule for adaptive sampling, especially since we measure frequencies but need to supply the STD with respect to the roller position. For this reason, we decided to set an STD equal to the percentage error found in the frequency domain as shown in Eqn. 3.

$$\sigma = \frac{\omega_{near}^{\text{previous}} - \omega_{meas}^{\text{current}}}{\omega_{meas}^{\text{current}}} \qquad (3)$$

Here, σ is an STD of a Gaussian distribution for location sampling, ω_{meas} is a measured resonant frequency, and ω_{near} is the closest frequency to the ω_{meas} among the fundamental frequencies. The superscripts *previous* and *current* are included in Eqn. 3 to strictly show that the samples are selected based on the estimate found from the previously measured frequency. Therefore, adaptive sampling depends on the current frequency measurement, as well as the modal frequencies selected relative to the frequency measured in the previous time step. Moreover, it is worth noting that, Eqn. 3 assumes that the frequency percentage error is equivalent to the position percentage error, but in reality, the two cannot be equal since position scale increments linearly whereas frequency scale does not.

The number of location samples can be assigned based on parallel computing capability. Assuming parallel computing is applicable, modal analysis on the FEA models can be performed on a single CPU or GPU thread. Therefore, with a large parallel computing resources, many location samples can be processed, possibly allowing better estimating performance even with a large STD. However, for this work 6 location samples are applied, assuming they can be computed in parallel.

Two different methods are implemented to estimate the current roller location, these are nearest neighbor and bounded regression. The nearest neighbor approach simply compares all natural frequencies with the measured frequency to find the closest one and selects the corresponding location as the current roller location. The bounded regression method finds a linear regression model that best represents the relation between the roller location and the frequency difference between the fundamental and resonant frequencies. Equation 4 gives the linear model fit by least-squares [13].

$$\begin{bmatrix} a \\ b \end{bmatrix} = (X^{\text{T}}X)^{-1}X^{\text{T}}Y, \text{ and } Y = \begin{bmatrix} \omega_1 - \omega_{\text{meas}} \\ \vdots \\ \omega_{\text{n}} - \omega_{\text{meas}} \end{bmatrix}, X = \begin{bmatrix} x_1 & 1 \\ \vdots & \vdots \\ x_{\text{n}} & 1 \end{bmatrix} \quad (4)$$

where ω is a fundamental frequency, ω_{meas} is a measured resonant frequency, x is a sampled location, n is a total number of samples, and (a, b) are regression parameters such that $\omega - \omega_{\text{meas}} = ax + b$. Since our goal is to find x when $\omega = \omega_{\text{meas}}$, the current roller location (x_{c}) is predicted as:
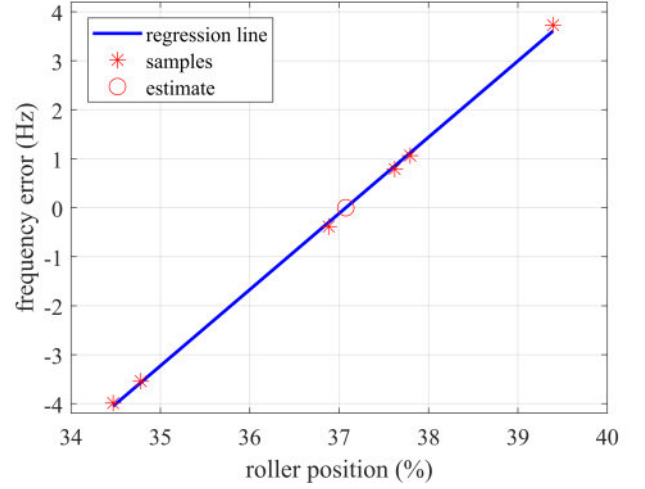
FIGURE 7. REGRESSION FOR ROLLER POSITION ESTIMATION.

$$x_{\text{c}} = \begin{cases} x_{\min} & \frac{-b}{a} < x_{\min} \\ x_{\max} & \frac{-b}{a} > x_{\max} \\ \frac{-b}{a} & \text{elsewhere} \end{cases} \qquad (5)$$

where, $x_{\min}$ and $x_{\max}$ are minimum and maximum roller locations of the samples. This indicates that the prediction is bounded within the range of samples, thus naming this algorithm as a bounded regression. The estimate is restricted to be within the sample range because errors in the regression model propagates more as we move further away from the samples. This way we can avoid the error by extending the regression model further away from the sample range. Fig. 7 displays how the bounded regression method works given 6 number of samples. From the figure, the asterisks and the circle represent the samples and the position estimate. The position estimate is simply the horizontal component of the point where the regression line crosses the zero frequency error.

In sum, the nearest neighbor method is a more robust approach, whereas the bounded regression method allows for more freedom in estimating the roller location since the roller location does not need to be equal to one of the sampled locations and consequently allows for smooth predictions.

RESULTS AND DISCUSSION

The experiment on the testbed has been performed with the proposed real-time updating scheme. Results of fixed and adaptive sampling are presented in separate sections. Within each
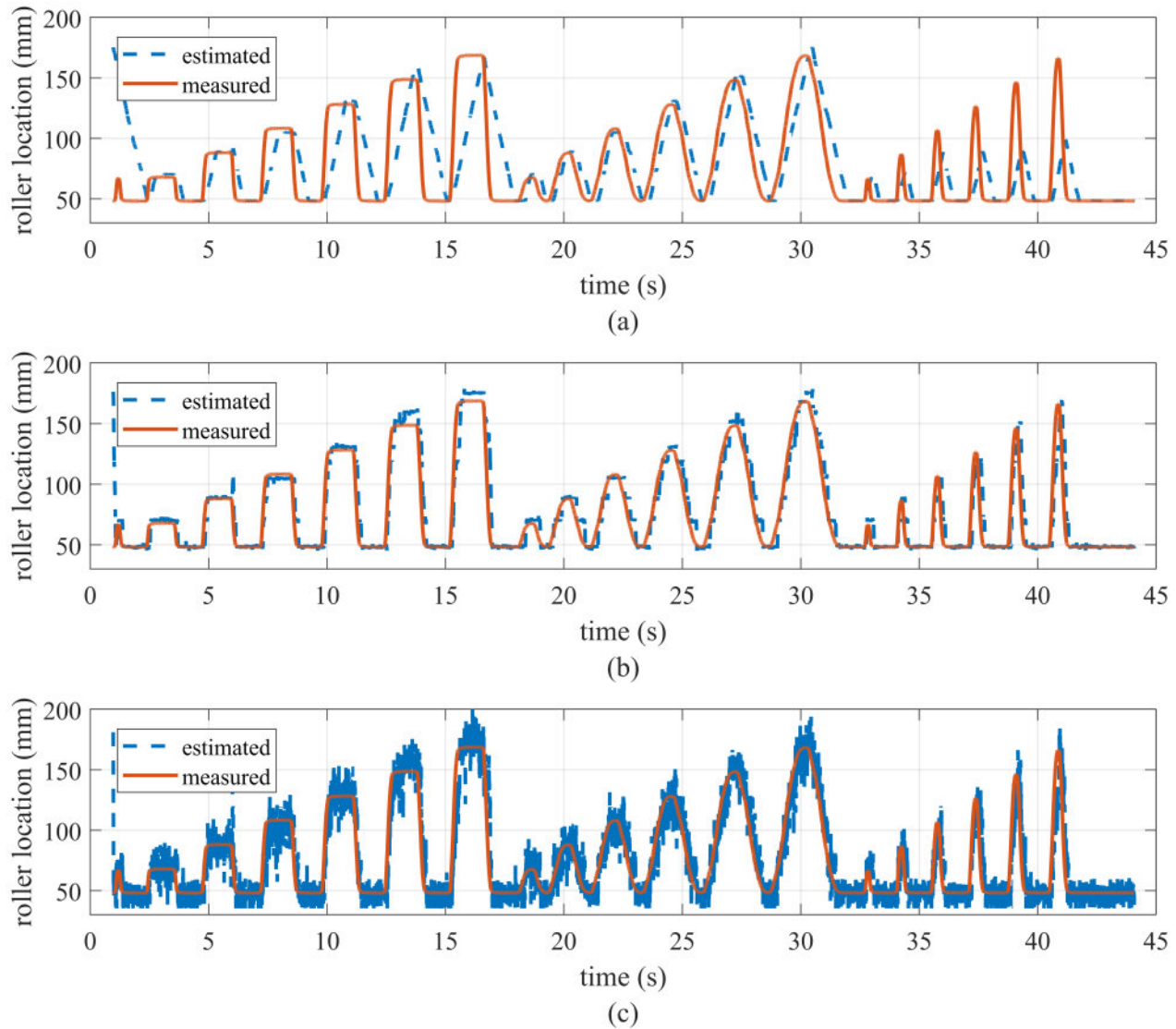
FIGURE 8. NEAREST NEIGHBOR ESTIMATIONS OF ROLLER LOCATION WITH DIFFERENT STANDARD DEVIATIONS: 0.1% (a), 1.0% (b), 10.0% (c).

section, STDs and roller position are presented in percentage instead of length. For instance, 1% refers to 1% of the total length of the beam. For fixed sampling, 0.1%, 1.0%, and 10.0% STDs are applied. For both sampling methods, nearest neighbor and bounded regression estimation approaches are compared.

Fixed Sampling

Figure 8 and Fig. 9 show the results of roller position estimations by fixed sampling with nearest neighbor and bounded regression approaches, respectively. Note that the offset in the estimated roller position at the start of each trial is due to setting

the initial conditions as the center of the beam (175mm). From both set of graphs, we can readily observe the effects of varying STD. As the STD increases, the search space (or sampling space) becomes larger so the samples are selected with larger variations. This causes the estimates to fluctuate more severely but allows faster convergence. For instance, 0.1% STD case reveals smooth solutions but manifests large delays. This delay prevents estimation during the high-rate dynamic interval shown in Fig. 8 and Fig. 9 between 32 and 45 seconds, such that the estimations cannot keep up with the actual changes in the system. This is because the range of selected samples is small so the
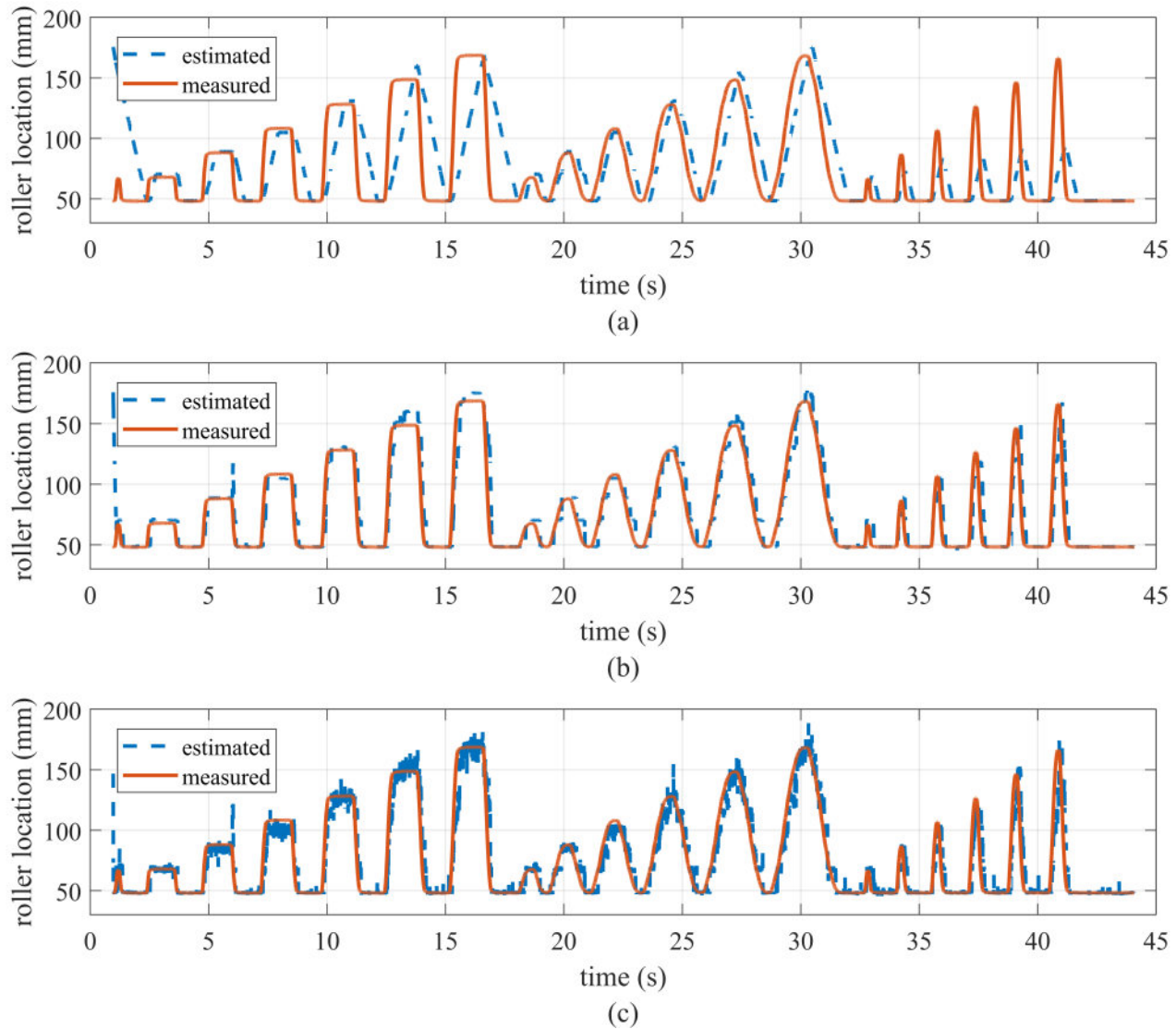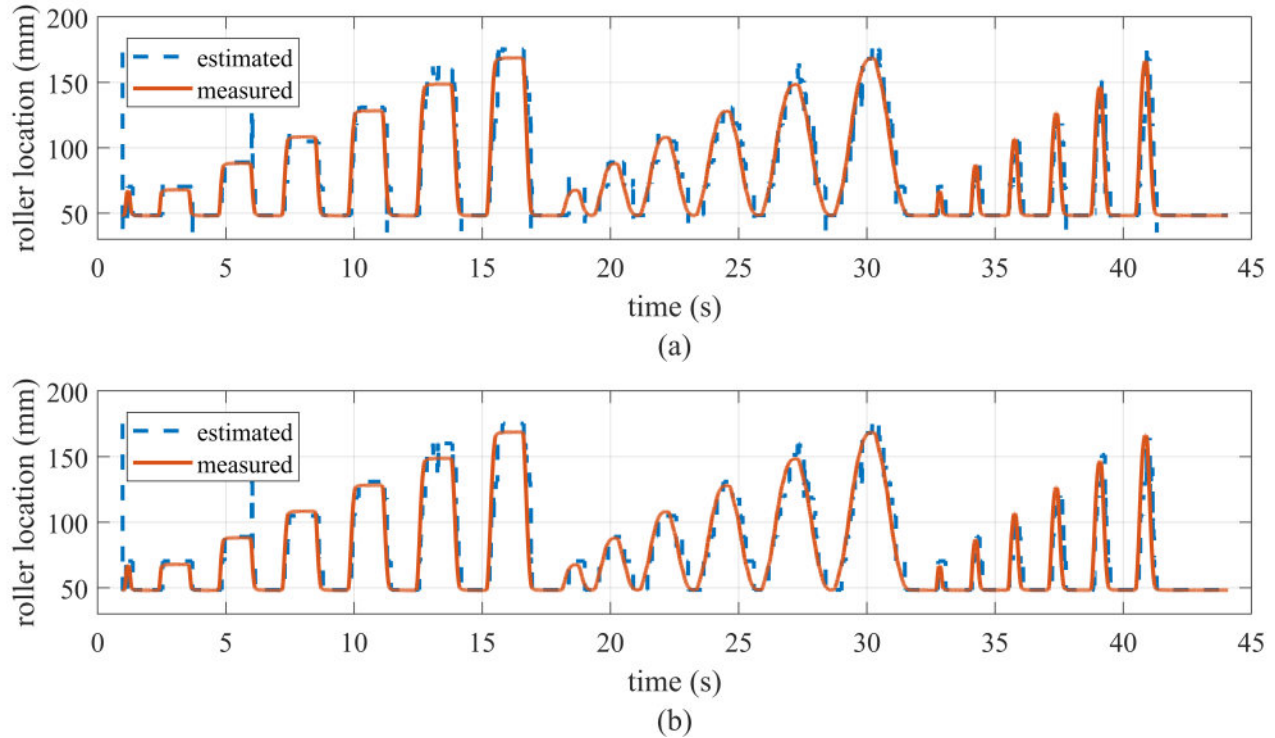
FIGURE 9. BOUNDED REGRESSION ESTIMATIONS OF ROLLER LOCATION WITH DIFFERENT STANDARD DEVIATIONS: 0.1% (a), 1.0% (b), 10.0% (c).

estimates, which are within the sampled range, remain far from the actual roller position until the roller moves back to within the sampled range. On the other hand, 10% STD allows to converge faster but produces excessive fluctuations according to the graphs. As expected, bounded regression does not help the convergence rate since the estimates are limited to be made within the sampled range. However, by comparing the two figures, we can visualize that the fluctuations of estimations decrease for 1% and 10% STD cases since by applying regression, the estimates are not necessarily equal to one of the sampled locations. The absolute mean error (AME) for each case of fixed sampling is presented in Table 1. Surprisingly, the solution for 10% STD is not very different from 1% STD. In fact, for the bounded regression algorithm, the solution for 10% STD is found to be more accurate than 1% STD. The only explanation for this is that, although not visible, since the convergence rate is faster for larger STD, the instantaneous error near the large slopes are much smaller such that the entire AME becomes smaller. Nevertheless, considering the smoothness and accuracy of the estimates bounded regression approach with 1% STD seems to be the best option.

FIGURE 10. ROLLER ESTIMATIONS WITH ADAPTIVE SEARCH SPACE USING NEAREST NEIGHBOR (a) AND BOUNDED REGRESSION (b).

TABLE 1. ABSOLUTE MEAN ERROR OF ROLLER ESTIMATIONS FOR FIXED SAMPLING (mm).

	Standard Deviation		
	0.1%	1.0%	10.0%
Nearest Neighbor	24.41	7.50	9.62
Bounded Regression	20.42	7.28	7.78

TABLE 2. ABSOLUTE MEAN ERROR OF ROLLER ESTIMATIONS FOR ADAPTIVE SAMPLING (mm).

Nearest Neighbor	Bounded Regression
6.91	6.90

Adaptive Sampling

The results of roller position estimates using adaptive search space are displayed in Fig. 10. Compared to fixed sampling results shown in Fig. 8 and Fig. 9 the estimates are smooth without apparent delays. For the nearest neighbor approach, sharp transient errors are visible near the rising and falling instances. This is the result of increasing the search space when large variations are applied, such that, although the nearest sample is selected, the sample still exhibits comparably large error. This phenomenon disappears when the bounded regression is applied along with the adaptive sampling. Although the variance increases due to a large difference in frequencies, estimates are found anywhere within the sampled range through the regression, thus allowing fewer fluctuations even for a large STD. In other words, even if the search space increases, the regression reduces the fluctuation, allowing smooth and accurate predictions. The AME for the two estimating approaches using adaptive search space are shown in Table 2. Numerically, the accuracy of the two approaches are almost identical. However, from the figure, we can clearly infer that the bounded regression delivers a better solution with adaptive sampling.

CONCLUSION

Roller estimations were calculated by fixed and adaptive sampling using both nearest neighbor and bounded regression approaches. Fixed sampling using the nearest neighbor approach

yields a direct relationship between STD and fluctuation as well as the rate of convergence. With low STD values yielding accurate values but lagging estimations and high STD values yielding real-time estimations with greater fluctuation in estimated values. Fixed sampling using bounded regression increases the accuracy of estimations by decreasing the fluctuation at all STD values compared to the nearest neighbor approach. The adaptive search space yields smoother results with fewer delays when compared to fixed sampling as a whole. Adaptive sampling using the nearest neighbor approach results in sharp transient errors directly after roller movement occurs, but the phenomenon disappears when the bounded regression is applied by decreasing the fluctuation of estimated values. From this work, it can be inferred that adaptive search spaces using bounded regression provides a viable method for updating FEA models in real-time.

REFERENCES

[1] Hong, J., Laflamme, S., Dodson, J., and Joyce, B., 2018. "Introduction to state estimation of high-rate system dynamics". *Sensors, 18(1):217*.

[2] Mostert, F. J., 2018. "Challenges in blast protection research". *Defense Technology*, pp. 1–7.

[3] Hong, J., Laflamme, S., and Dodson, J., 2018. "Study of input space for state estimation of high-rate dynamics". *Structural Control Health Monitoring, 25*, pp. 1–14.

[4] Song, W., and Dyke, S., 2014. "Real-time dynamic model updating of a hysteric structural system". *Journal of Structural Engineering, 140*, pp. 1–14.

[5] Downey, A., Hong, J., Dodson, J., Carroll, M., and Scheppegrell, J., 2020. "Millisecond model updating for structures experiencing unmodeled high-rate dynamic events". *Mechanical Systems and Signal Processing, 138*, apr, p. 106551.

[6] Reddy, J. N., 2006. *An Intro to the Finite Element Method*. McHraw Hill.

[7] Li, L., and Bettess, P. "Adaptive finite element methods: A review". *ASME Applied Mechanics Reviews, volume = 50, pages = 581-591, year = 1997.*

[8] Huang, W., and Russell, R., 2001. "Adaptive mesh movement — the mmpde approach and its applications". *Journal of Computational and Applied Mathematics, 128*, pp. 383–398.

[9] Budd, C., Collins, G., Huang, W., and R.D.Russell, 1998. "Self-similar numerical solutions of the porous-medium equation using moving mesh methods". *Philosophical Transactions of the Royal Society A Mathematical Physical and Engineering Sciences*, pp. 1047–1077.

[10] Cao, W., Huang, W., and Russell, R., 1999. "An r-adaptive finite element method based upon moving mesh pdes". *Journal of Computational Physics, 149*, pp. 221–244–7.

[11] Oden, J., Strouboulis, T., and Devloo, P., 1986. "Adaptive finite element methods for the analysis of inviscid compressible flow: Part i. fast refinement/ unrefinement and moving mesh methods for unstructured meshes". *Computer Methods in Applied Mechanics and Engineering, 59*, pp. 327–362.

[12] Joyce, B., Dodson, J., Laflamme, S., and Hong, J., 2018. "An experimental test bed for developing high-rate structural health monitoring methods". *Shock and Vibration, 2018*, pp. 1–10.

[13] Hastie, T., R.Tibshirani, and Friedman, J. *The Elements of Statistical Learning*. Springer.